Neuroradiology
https://doi.org/10.1007/s00234-022-02924-x

FUNCTIONAL NEURORADIOLOGY

# Converging evidence of impaired brain function in systemic lupus erythematosus: changes in perfusion dynamics and intrinsic functional connectivity

**Efrosini Papadaki[1,2] · Nicholas J. Simos[2,3] · Eleftherios Kavroulakis[1] · George Bertsias[4,5] · Despina Antypa[6] · Antonis Fanouriakis[4,7] · Thomas Maris[1,2] · Prodromos Sidiropoulos[4] · Dimitrios T Boumpas[4,7,8,9]**

Received: 12 November 2021 / Accepted: 24 February 2022


## Abstract

**Purpose** The study examined changes in hemodynamics and functional connectivity in patients with systemic lupus erythematosus (SLE) with or without neuropsychiatric manifestations.

**Methods** Participants were 44 patients with neuropsychiatric SLE (NPSLE), 20 SLE patients without such manifestations (non-NPSLE), and 35 healthy controls. Resting-state functional MRI (rs-fMRI) was used to obtain whole-brain maps of (a) perfusion dynamics derived through time shift analysis (TSA), (b) regional functional connectivity (intrinsic connectivity contrast (ICC) coefficients), and (c) hemodynamic-connectivity coupling. Group differences were assessed through independent samples *t*-tests, and correlations of rs-fMRI indices with clinical variables and neuropsychological test scores were, also, computed.

**Results** Compared to HC, NPSLE patients demonstrated intrinsic hypoconnectivity of anterior Default Mode Network (DMN) and hyperconnectivity of posterior DMN components. These changes were paralleled by elevated hemodynamic lag. In NPSLE, cognitive performance was positively related to higher intrinsic connectivity in these regions, and to higher connectivity-hemodynamic coupling in posterior DMN components. Uncoupling between hemodynamics and connectivity in the posterior DMN was associated with worse task performance. Non-NPSLE patients displayed hyperconnectivity in posterior DMN and sensorimotor regions paralleled by relatively increased hemodynamic lag.

**Conclusion** Adaptation of regional brain function to hemodynamic changes in NPSLE may involve locally decreased or locally increased intrinsic connectivity (which can be beneficial for cognitive function). This process may also involve elevated coupling of hemodynamics with functional connectivity (beneficial for cognitive performance) or uncoupling, which may be detrimental for the cognitive skills of NPSLE patients.

**Keywords** Neuropsychiatric lupus · Resting-state fMRI · Cerebral perfusion · Time shift analysis · Intrinsic connectivity coefficient · Visuomotor capacity

## Introduction

Systemic lupus erythematosus (SLE) is a systemic autoimmune inflammatory disorder which often affects the CNS [1]. Symptoms vary widely among patients with neuropsychiatric SLE (NPSLE), ranging from overt (e.g., seizures, psychosis) to subtle presentations, such as headache, depression and anxiety symptoms, and cognitive dysfunction [2]. Microscopic brain lesions, not detectable by conventional brain MRI, have been found in over 50% of NPSLE patients in histopathological studies [3]. The development of novel, advanced MRI techniques has improved sensitivity to detect hemodynamic changes, as well as functional alterations as indexed by functional brain connectivity. Few MR perfusion imaging studies using dynamic susceptibility contrast (DSC) [4–8] or arterial spin labeling (ASL) [9, 10] reported regional hemodynamic changes in SLE patients without (non-NPSLE) or with (NPSLE) neuropsychiatric clinical manifestations, ranging from non-significant [4, 5] to hypoperfusion [6, 9, 10] or even hyperperfusion [7, 8, 10]. However, the significance of altered perfusion dynamics in

✉ Efrosini Papadaki
fpapada@otenet.gr

Extended author information available on the last page of the article

Published online: 06 March 2022

specific brain regions for neuronal function and functional connectivity with other brain areas has not been explored.

Resting-state functional MRI (rs-fMRI) is a noninvasive imaging technique, using blood oxygenation level-dependent (BOLD) signal, which has been widely used to investigate the functional deficits in various CNS diseases. Studies in patients with SLE with or without neuropsychiatric symptoms have reported altered functional connectivity was shown both within and between several key brain networks [11–21]. Interestingly, rs-fMRI could provide evidence not only about neural activity, but also about regional cerebral perfusion alterations, through time-shift analysis (TSA), a promising new method that has been used to assess hemodynamics in previous studies [22–29]. According to this method, the hemodynamic transfer speed is indexed through the temporal shift of low-frequency BOLD signal fluctuations of rs-fMRI. A disturbance of local blood flow is reflected in these fluctuations as a localized delay (i.e., hemodynamic lag) or temporal gain (i.e., hemodynamic lead) in relation to the blood flow in major cerebral veins. Substantial shifts, in the order of seconds, have been shown to provide information about local brain hemodynamics similar to established MR perfusion techniques [25, 27, 28].

To this date, this technique has been applied not only to neurological conditions characterized by severe perfusion disturbances, such as stroke [22–24, 27, 28] but, also, in patients with Alzheimer's dementia or mild cognitive impairment displaying smaller variations of hemodynamic impairment [29]. More recently, whole-brain TSA and intrinsic connectivity contrast (ICC) maps were computed in a group of NPSLE patients to identify potential correlated with emotional disturbances which are quite common in this disorder. We showed that anxiety and depression symptom severity was associated with accelerated hemodynamic response in limbic and ventromedial orbitofrontal regions, respectively [30]. These changes were paralleled by reduced intrinsic connectivity in dorsolateral prefrontal and medial orbitofrontal regions, respectively. In this context, potential interdependencies between relative subtle hemodynamic disturbances and regional brain function, as indexed by the overall degree of connectivity of a given region with the rest of the brain, have not been explored systematically. For instance, is overall functional connectivity of a given region reduced when venous drainage of this region is delayed by several seconds? Conversely, when venous drainage in a given region is accelerated, is functional connectivity of increased accordingly?

In the present study, we integrated estimates of regional hemodynamic status with indices of functional connectivity derived from rs-fMRI data in non-NPSLE and NPSLE patients and healthy age- and gender-matched controls. These indices were studied separately, as well as in combination through anatomical overlay maps, to explore the possible hemodynamic alterations underlying functional connectedness changes in patients with SLE. In addition, the potential functional significance of such changes for the clinical and cognitive status of non-NPSLE and NPSLE patients was addressed through correlational analyses.

## Methods

### Participants

Patients diagnosed with NPSLE ($n = 44$) or non-NPSLE ($n = 20$), who regularly visited the outpatient clinic of the University Hospital of Heraklion and met the inclusion criteria, were invited to participate in the study by their attending physician. All patients met the revised ACR 1997 classification criteria for SLE [31]. NPSLE diagnosis was based on physician judgment, following multidisciplinary approach and considering patient age and risk factors for NPSLE (anti-phospholipid antibodies, prior neuropsychiatric manifestation, generalized disease activity, findings of conventional MRI imaging, and other diagnostic procedures). Additional inclusion criteria were age over 18 years, negative history of thromboembolic cardiovascular disease, or other primary CNS diseases.

As shown in Table 1, the vast majority of SLE patients were women, aged 19 to 65 years (IQR = 37.3–54 years) ranging between 1 and 25 years since SLE diagnosis (IQR = 2.0 to 9.3 years). The majority of patients presented with relatively mild disease activity (only 5 patients had SLEDAI scores $\geq 9$) and organ damage at the time of testing (only 3 patients had SLICC scores $\geq 1$).

Comparison rs-fMRI data were available on 35 age- ($p > .1$) and gender-matched ($p > .4$) healthy volunteers (HC) (see Table 1). The hospital review board approved the study, and the procedure was thoroughly explained to all patients and volunteers who signed informed consent.

### Laboratory parameters, disease activity, and neuropsychological tests

Relevant laboratory tests, including antiphospholipid antibodies, ESR, CRP, C3, and C4, were performed at the time of assessment. The SLE Disease Activity Index (SLEDAI-2000) was used to assess disease activity [32] and the Systemic Lupus International Collaborating Clinics/American College of Rheumatology (SLICC/ACR) Damage Index (SDI) for organ damage [33]. Neuropsychological testing was performed on 35 NPSLE patients specifically aiming to include tests recommended by the ACR [34] (described in more detail in the Supplementary Material). Corresponding neuropsychological data were available on only 12 non-NPSLE patients which were not sufficient for correlational analyses.

**Table 1** Demographic and clinical characteristics of lupus patients and healthy comparison group (HC)

| *n* | NPSLE<br>44 | non-NPSLE<br>20 | HC<br>35 | *p* value |
|---|---|---|---|---|
| Female | 42 (95.5%) | 19 (95.0%) | 32 (91.4%) | .1 |
| Age, mean (SD in years) | 43.8 (12.5) | 48.4 (13.6) | 42.9 (15.4) | .4 |
| Disease duration, mean (SD in years) | 6.3 (6.2) | 6.1 (6.7) | – | .8 |
| Neuropsychiatric manifestation | | | – | – |
| ■ Mood disorder | 8 | | | |
| ■ Depression | 4 | | | |
| ■ Anxiety disorder | 8 | | | |
| ■ Cognitive disorder | 8 | | | |
| ■ Lupus headache | 8 | | | |
| ■ Psychosis | 3 | | | |
| ■ Cranial neuropathy | 2 | | | |
| ■ Peripheral neuropathy | 1 | | | |
| ■ Stroke[a] | 4 | | | |
| ■ DVT | 1 | | | |
| ■ Seizures | 2 | | | |
| SLEDAI, mean (SD) | 4.5 (3.0) | 4.5 (3.07) | – | .8 |
| SLICC/ACR score, mean (SD) | 0.34 (0.57) | 0.35 (0.93) | – | .7 |
| aPL (+)ve | 4 (9.1%) | 4 (20.0%) | – | .1 |
| Treatments | | | – | – |
| ■ Antiplatelets | 7 (15.9%) | – | – | |
| ■ Anticoagulants | 1 (2.3%) | 1 (10.0%) | – | |
| ■ Antihypertensives | 12 (27.3%) | 1 (10.0%) | – | |
| ■ Glucocorticoids | 21 (47.8%) | 11 (55.0%) | – | |
| ■ Immunosuppressives | 26 (59.0%) | 9 (45.0% | – | |
| ■ Biologics | 3 (6.8%) | – | – | |
| Smoking | 17 (38.6%) | 6 (30.0%) | 12 (34.3%) | .4 |
| Significant depression symptoms[b] | 18 (40.9%) | 4 (20.0%) | 6 (17.1%) | .04 |

*NPSLE* neuropsychiatric SLE, *SLEDAI* Systemic Lupus Erythematosus Disease Activity Index, *SLICC* Systemic Lupus International Collaborating Clinics, *ACR* American College of Rheumatology

[a]Without overt athero-thrombotic disease or MRI lesions. NPSLE vs. non-NPSLE: $p = .1$, NPSLE vs. HC: $p = .002$, HC vs. non-NPSLE: $p = .2$

[b]As indicated by scores > 8 points on the HADS Depression subscale; NPSLE vs non-NPSLE: $p = .1$, NPSLE vs. HC: $p = .01$

## MR imaging

Brain MRI examinations were performed on a clinical 1.5 T whole-body superconducting imaging system (Vision/Sonata, Siemens/Erlangen), equipped with high-performance gradients (gradient strength: 40 mT/m, slew rate: 200 mT/m/ms) and a two-element circularly polarized head array coil. Conventional MR imaging protocol consisted of a 3D T1-w MPRAGE, a T2wTSE, and a Turbo FLAIR sequence. Images were interpreted by a senior neuroradiologist (XX), with 20 years of experience, blinded to the clinical and laboratory data, who reported any incidental findings not related to SLE, or findings related to focal SLE-related abnormalities, such as acute or old infarcts, hemorrhages, and focal brain atrophy. Patients with any of the aforementioned MRI findings were excluded from the study.

Rs-fMRI was derived from a T2*-weighted, fat-saturated 2D-FID-EPI sequence (TR = 2300 ms, TE = 50 ms, FOV = 192 × 192 × 108 mm. Acquisition voxel size was 3 × 3 × 3 mm, and whole brain scans consisted of 36 transverse slices acquired parallel to the plane passing through the anterior and posterior commissures (AC-PC line with 3.0-mm slice thickness and no interslice gap).

### fMRI data preprocessing and denoising

Each BOLD time series consisted of 150 dynamic volumes (the first three were ignored in all subsequent analyses). Preprocessing steps included slice-time correction, realignment, segmentation of structural data, normalization into standard stereotactic Montreal Neurological Institute (MNI) space, and spatial smoothing using a Gaussian kernel of 8-mm

full-width at half-maximum using SPM8. As functional connectivity is affected by head motion in the scanner, we accounted for motion artifact detection and rejection using the artifact detection tool (ART; http://www.nitrc.org/projects/artifact_detect). White matter and cerebrospinal fluid signal (CSF) mean signals were regressed out of all voxel time series in order to mitigate their effects on fMRI BOLD time courses. The first five principal components of white matter and CSF regions were regressed out of the signal as well as their first-order derivatives. These steps were completed using CompCor implemented within the CONN preprocessing module [35] and executed in MATLAB. The fMRI time series were detrended and bandpass filtered in the 0.008–0.09 Hz range, to eliminate low-frequency drift and high-frequency noise [30].

#### Time shift analysis

After fMRI data preprocessing and denoising whole-brain TSA maps were calculated as described in several previous studies [22–25, 30] using in house MATLAB scripts. It should be noted that for the calculation of TSA, only the CSF signal was regressed out of the BOLD fMRI time courses, while all the remaining preprocessing steps were applied as described above. Global grey and white matter signals are not considered noise in the calculation of TSA, and thus, their influence on the voxel time series was not removed [30]. Firstly, a mask of the major venous sinuses was created based on the standard brain. The reference BOLD time series was calculated as the mean of all the voxel time series included in the venous mask. Then, voxel-wise cross correlations were calculated in reference to this regressor for lags of − 3 TRs to 3 TRs (or − 6.96 to 6.96 s). This entails the computation of the lagged versions of each voxel time series (− 3 TR to 3 TR) and of the correlation coefficient of each lagged version of the time series with the reference signal. The lag value corresponding to the highest correlation coefficient was then assigned to each voxel as its time shift value. In this manner, in each subject's TSA map, each voxel value represents the lag or lead of that voxel's BOLD activity relative to the average signal extracted from the venous sinuses.

#### Voxel-wise functional connectivity

Voxel-wise global connectivity was assessed through the intrinsic connectivity contrast (ICC) an estimate of the degree of association between the time-series of a given voxel with all the remaining voxels in the brain (in the present study, voxels included in all 90 cortical regions of the Automated Anatomical Atlas (AAL) atlas). All preprocessing steps described in "fMRI data preprocessing and denoising" were implemented prior to voxel level ICC computation. MATLAB code for the calculation of ICC maps using Singular Value Decomposition, similar to the implementation found in CONN [35], is freely available online [36]. ICC is conceptually similar to the graph-theoretical measure of degree. Degree signifies the number of regions connected to each individual region, while the calculation of ICC, on a weighted network, takes into account the connectivity strengths of all connections present for each voxel. Specifically, a voxel's ICC value is computed as the mean of that voxel's time series correlation values with all other voxels' time series, squared.

#### Connectivity-hemodynamic coupling

We also computed two separate voxel-wise overlay masks: one comprising voxels displaying coupling between hemodynamics and intrinsic connectivity, and the second comprising voxels that showed uncoupling. The former comprised voxels displaying significant ICC ($p < .001$ uncorrected in first-level analyses) coupled with hemodynamic lead, as indicated by TSA values $< -1$ TR, whereas the latter comprised voxels displaying significant ICC combined with hemodynamic lag (TSA values $> 1$ TR). The integration of ICC and TSA metrics was implemented by overlaying binary voxel maps created using the statistic thresholds mentioned above at the subject level. The first map contains only voxels with concurrently high global connectivity and hemodynamic lead (hyperperfusion) while the latter increased global connectedness and hemodynamic lag (hypoperfusion). These two opposite combinations of the measures were calculated in order to examine the direction of their relationship, i.e., whether hyperconnected regions were relatively hypo- or hyper-perfused.

#### Correlations with neuropsychological measures

Correlations of clinical variables and neuropsychological test scores were computed with ICC, TSA, and ICC-TSA coupling indices. Hemodynamic and connectivity indices used in these analyses were restricted to voxel clusters and corresponding aal atlas regions, where significant group differences were found.

Regarding ICC and TSA data, four complementary indices were computed. The first reflected average TSA or ICC values within spherical ROIs (10 mm in diameter) centered at the voxel with peak value in the pairwise group comparisons (geometric cluster center coordinates are listed in Tables 2 and 3). We also computed voxel percentages within corresponding aal atlas regions to accommodate individual differences in the precise anatomical location of cluster peak coordinates. According to this approach, first, we identified the aal atlas region comprising the peak of each cluster of significant between-group differences. Then, we calculated three different measures for each selected aal region: (i)

**Table 2** Results of paired *t* tests comparing the study groups on TSA values

| Brain region | MNI coordinates (x y z) | Brain region | MNI coordinates (x y z) | Brain region | MNI coordinates (x y z) |
|---|---|---|---|---|---|
| **NPSLE > HC** | | **Non-NPSLE > HC** | | **Non-NPSLE> NPSLE** | |
| R precuneus | 10 − 61 66 | R precuneus | 9 − 59 56 | L IPL | − 38 − 43 41 |
| L precuneus | − 5 − 62 67 | L precuneus | − 7 − 57 59 | R postcentral | 46 − 22 41 |
| R SMA | 6 − 4 61 | R PCL | 5 − 51 66 | L postcentral | − 53 − 25 41 |
| L SMA | − 4 − 18 65 | L PCL | − 6 − 45 65 | R TP | 47 14 − 37 |
| R MCC (BA24) | 3 5 38 | R SMA | 6 − 27 70 | L pMTG | − 46 − 63 22 |
| L MCC (BA24) | − 6 − 7 38 | L SMA | − 4 − 21 70 | | |
| R SPL | 12 − 55 66 | R postcentral | 62 − 25 38 | | |
| R SMG | 63 − 28 27 | L postcentral | − 63 − 21 28 | | |
| R insula (BA13) | 43 14 4 | | | | |
| **HC > NPSLE** | | **HC > non-NPSLE** | | **NPSLE > non-NPSLE** | |
| R MOG | 40 − 84 14 | R mOFC (BA10) | 18 61 6 | L caudate | − 10 19 − 2 |
| L pMTG | − 33 − 81 4 | L mOFC (BA10) | − 4 58 5 | L putamen | − 22 8 − 2 |
| L mOFC (BA10) | − 19 56 14 | | | | |

All effects remained significant after controlling for age

*SMA* Supplementary Motor Area, *MCC* Middle Cingulate Cortex, *SPL* Superior Parietal Lobule, *SMG* supramarginal gyrus, *MOG* middle occipital gyrus, *pMTG* posterior middle temporal gyrus, *mOFC* medial orbitofrontal cortex, *PCL* paracentral lobule, *IPL* inferior parietal lobule, *TP* temporal pole

**Table 3** Results of paired t-tests comparing the study groups on ICC

| Brain region | MNI coordinates (x y z) | Brain region | MNI coordinates (x y z) | Brain region | MNI coordinates (x y z) |
|---|---|---|---|---|---|
| **NPSLE > HC** | | **Non-NPSLE > HC** | | **Non-NPSLE > NPSLE** | |
| R precuneus | 23 − 82 41 | R precuneus | 8 − 51 56 | R precuneus | 12 − 63 48 |
| L precuneus | − 28 − 71 38 | L precuneus | − 4 − 56 57 | L precuneus | − 5 − 60 43 |
| R SPL | 23 − 71 47 | R SPL | 30 − 56 59 | R SPL | 14 − 51 71 |
| L SPL | − 27 − 69 47 | L SPL | − 22 − 60 56 | L SPL | − 11 − 52 68 |
| L angular gyrus | − 41 − 68 36 | R angular gyrus | 49 − 60 41 | L angular gyrus | − 44 − 50 43 |
| | | L angular gyrus | − 41 − 61 40 | | |
| **HC> NPSLE** | | **HC > non-NPSLE** | | **Non-NPSLE < NPSLE** | |
| R TP | 46 7 − 38 | R TP | 48 12 − 39 | – | – |
| L TP | − 36 7 − 36 | L TP | − 40 13 − 35 | | |
| L SFG (BA9) | − 14 59 34 | | | | |
| L MFG (BA10/46) | − 45 46 20 | | | | |
| L vmPFC (BA10) | − 11 66 − 14 | | | | |
| R SFG (BA9) | 24 55 34 | | | | |
| R MFG (BA10/46) | 48 42 23 | | | | |
| R vmPFC (BA10) | 6 65 10 | | | | |

All effects remained significant after controlling for age

*SPL* superior parietal lobule, *SFG* superior frontal gyrus, *MFG* middle frontal gyrus, *vmFC* ventromedial prefrontal cortex, *TP* temporal pole

percentage of voxels with positive time delay values (> 1 TR) representing hemodynamic lag, (ii) percentage of voxels with negative time delay values (< − 1 TR) representing hemodynamic lead, and (iii) percentage of voxels with significant ICC values according to first level one-sample *t* tests ($p < .001$ uncorrected).

Finally, binary ICC-TSA overlay voxel maps were used to compute two additional complementary indices of coupling and uncoupling, respectively: (i) percentage of voxels displaying high ICC values and hemodynamic lead and (ii) percentage of voxels displaying high ICC values and hemodynamic lag.

### Statistical analysis

**Group comparisons** Whole-brain ICC and TSA maps were submitted to first- and second-level one-sample *t* tests in SPM12. The latter involved (a) one-sample *t*-tests performed separately for each participant group and (b) independent-samples *t*-tests comparing NPSLE vs HC, non-NPSLE vs HC and non-NPSLE vs NPSLE groups. Given that this is the first attempt to assess minimal hemodynamic changes combined with changes in nodal functional connectivity on a clinical sample, we employed a somewhat liberal statistical threshold of $p < .05$ (false discovery rate (FDR) corrected, which was used in a previous clinical study; 29). However, in order to further reduce the likelihood of finding spurious results, the additional criterion of a minimum cluster size of 200 voxels was imposed on all group comparisons. Minimum cluster size was computed via the Monte Carlo simulation method proposed by Slotnick et al. [37, 38] using the estimated smoothness of our functional data (10 mm). ICC-TSA coupling maps which were derived from a two-step thresholding procedure were compared between groups at a more liberal criterion of $p < .1$ FDR-corrected.

**Correlations with clinical test scores** Partial correlations were computed between each of the five indices described in "Correlations with neuropsychological measures" and (a) clinical data (disease duration, SLEDAI score) and (b) age- and education-adjusted neuropsychological test standard scores (based on population norms). Age served as a covariate in these analyses (with the exception of correlations with disease duration). These analyses were restricted to the group of NPSLE patients (given the insufficient group size of the non-NPSLE group for such analyses) and were performed using SPSS v. 20 (SPSS Inc., Chicago, IL, USA).

## Results

### Neurocognitive status of NPSLE patients

On average, NPSLE patients performed within one SD below the normative population average on all neuropsychological test indices, although a considerable percentage of patients (20%) scored in the significantly impaired range ($z < -1.5$) on at least three indices (see Supplementary Figure 1).

### Evidence of impaired hemodynamic status in NPSLE and non-NPSLE

Significantly higher TSA values in the NPSLE vs the HC group were found bilaterally in the supplementary motor area, precuneus, and middle cingulate cortex, and also in the right supramarginal gyrus, superior parietal lobule (SPL), and insula (Fig. 1b; Table 2). Inspection of the map of average TSA values in Fig. 1c reveals that NPSLE patients as a group displayed hemodynamic lag in all these areas (TSA > 1TR). Compared to the non-NPSLE group, NPSLE patients displayed significantly greater hemodynamic lag in the caudate and putamen (Fig. 1 e and f).

Pairwise contrasts in the opposite direction (HC > NPSLE) were found in lateral occipital cortices (right middle occipital gyrus), left posterior middle temporal gyrus, and left medial orbitofrontal cortex, where NPSLE patients displayed hemodynamic lead (Fig. 1c). Significant non-NPSLE > NPSLE contrasts were found bilaterally in the postcentral gyrus (Fig. 1 e and f) and also in the left inferior parietal lobule and adjacent posterior middle temporal gyrus, and in the right temporal pole. Inspection of Fig. 1e suggests that these regions demonstrated significant hemodynamic lag among non-NPSLE patients.

Significant non-NPSLE > HC contrasts were found bilaterally in the precuneus, paracentral lobule, supplementary motor area, and primary somatosensory cortex (Fig. 1d; Table 2). Inspection of the map of average TSA values in Fig. 1e reveals that non-NPSLE patients as a group displayed hemodynamic lag in all these areas (TSA > 1TR). Pairwise contrasts in the opposite direction (HC > non-NPSLE) were found in bilateral medial orbitofrontal cortex where non-NPSLE patients displayed hemodynamic lead.

*Evidence of aberrant whole-brain intrinsic connectivity in NPSLE and non-NPSLE*

Evidence of increased intrinsic connectivity among NPSLE patients as compared to HC participants was found mainly in parietal lobe regions, as shown by the results of one-sample *t* tests (indicating clusters of voxels displaying significant ICC in whole-brain analyses) as well as paired-sample *t*-tests (showing voxel clusters with significantly higher ICC in NPSLE vs HC groups) (Fig 2). Inspection of Table 2 indicates that regions displaying hyperconnectivity in NPSLE comprise the posterior portion of the DMN (precuneus, SPL, bilaterally, and the left angular gyrus). Conversely, reduced intrinsic connectivity was observed in anterior DMN components (ventromedial and superior prefrontal cortex and the temporal poles).

Non-NPSLE patients also displayed increased ICC, as compared to both the HC and NPSLE groups, in posterior DMN regions, although reduced intrinsic connectivity was restricted to the temporal poles.

### Coupling of intrinsic connectivity and hemodynamic disturbances in NPSLE and non-NPSLE

Compared to healthy controls, NPSLE patients displayed increased connectivity coupled with hemodynamic lead in the cuneus (bilaterally), right middle occipital, right

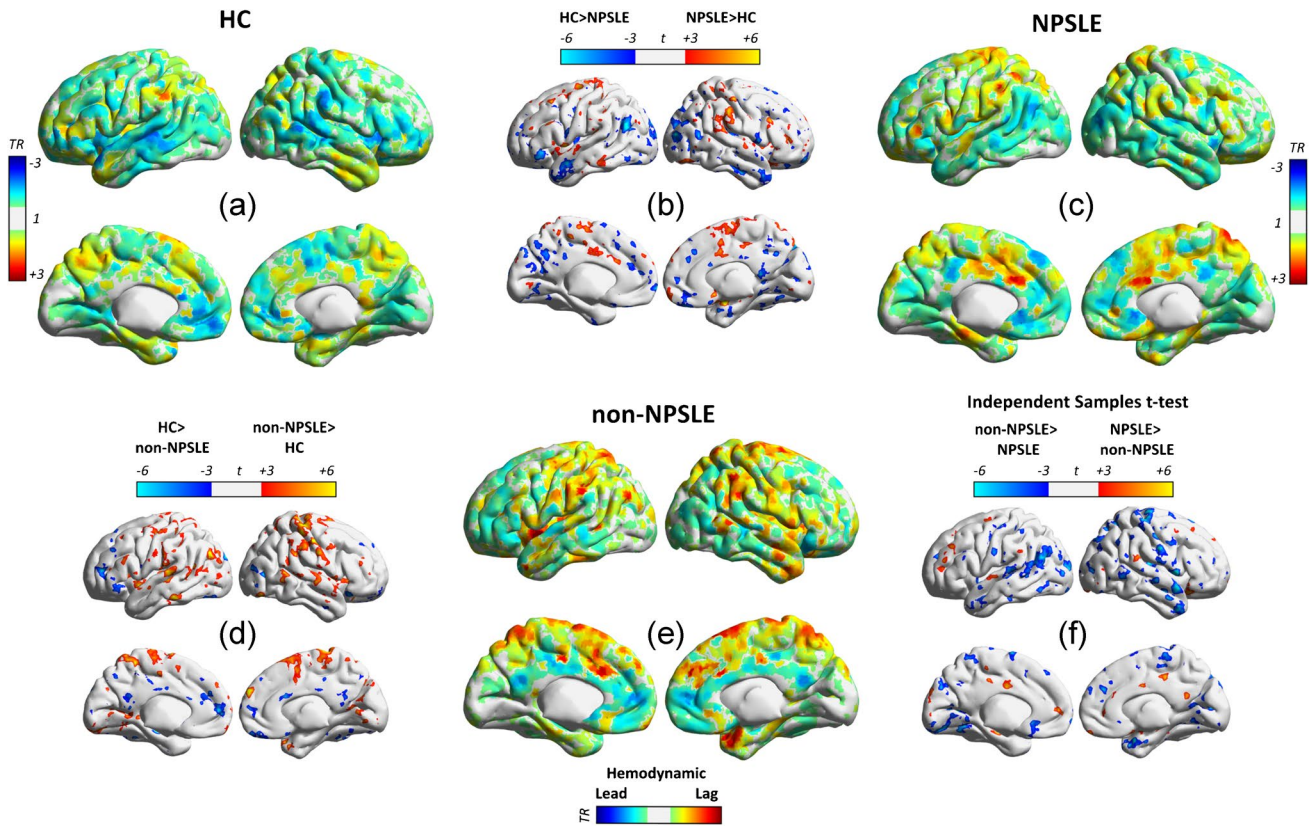


**Fig. 1** Whole-brain TSA maps. **a**, **c**, **e**: Group TSA maps in healthy controls (HC), non-NPSLE and NPSLE patients displaying voxels that showed hemodynamic lag (positive TSA values > 1 TR) or lead (negative TSA values < − 1 TR). **b**, **d**, **f**: Pairwise t-contrasts on parametric TSA maps between study groups (thresholded at $p < .05$, FDR corrected with minimum cluster size of 200 voxels)

posterior middle temporal gyrus, right angular gyrus, and right precentral gyrus (Fig 3). Conversely, increased uncoupling of ICC with hemodynamics (i.e., voxels displaying high ICC and hemodynamic lag) in NPSLE as compared to the HC group was found in the precuneus and adjacent SPL bilaterally. The non-NPSLE group showed reduced coupling in pericalcarine cortex and increased uncoupling in the precuneus, bilaterally, as compared to the HC group.

## Associations of clinical variables with hemodynamic and connectivity indices

Among NPSLE patients (as well as in the total sample of SLE patients), hemodynamic lag (% voxels displaying hemodynamic transfer lags > 1 TR) increased with longer disease duration in the right SMA ($r = .362$, $p = .019$) and paracentral lobule ($r = .368$, $p = .018$). Intrinsic connectivity was also positively related to disease duration in the left ($r = .418$, $p = .02$) and right SPL ($r = .502$, $p = .006$). Further, higher percentage of voxels in the right SPL displaying high ICC coupled with hemodynamic lag (> 1 TR) (TSA-ICC conjunction maps) was associated with greater impact of the disease (SLEDAI score adjusted for age; $r = .319$, $p = .03$).

## Associations of neuropsychological test scores with hemodynamic and connectivity indices in NPSLE

**Hemodynamics** Significant associations (age-adjusted) with neuropsychological test scores were found for hemodynamic lag in the right middle cingulate cortex (where NPSLE patients displayed higher hemodynamic lag than the HC group). Specifically, higher lag values among NPSLE patients correlated with worse performance on Digits Reverse ($r = -.34$, $p = .030$) and AVLT Delayed Recall ($r = -.49$, $p = .01$).

**Functional connectivity** Positive associations of immediate verbal memory scores with ICC, controlling for age, were found in both posterior (SPL) and anterior DMN regions (right SFG). Specifically, ICC in the left SPL correlated with AVLT Delayed Recall ($r = .486$, $p = .003$), ICC in the right SPL with AVLT Delayed Recall ($r = .551$, $p = .001$), and ICC in the right SFG with Digits Reverse ($r = .539$, $p = .001$).

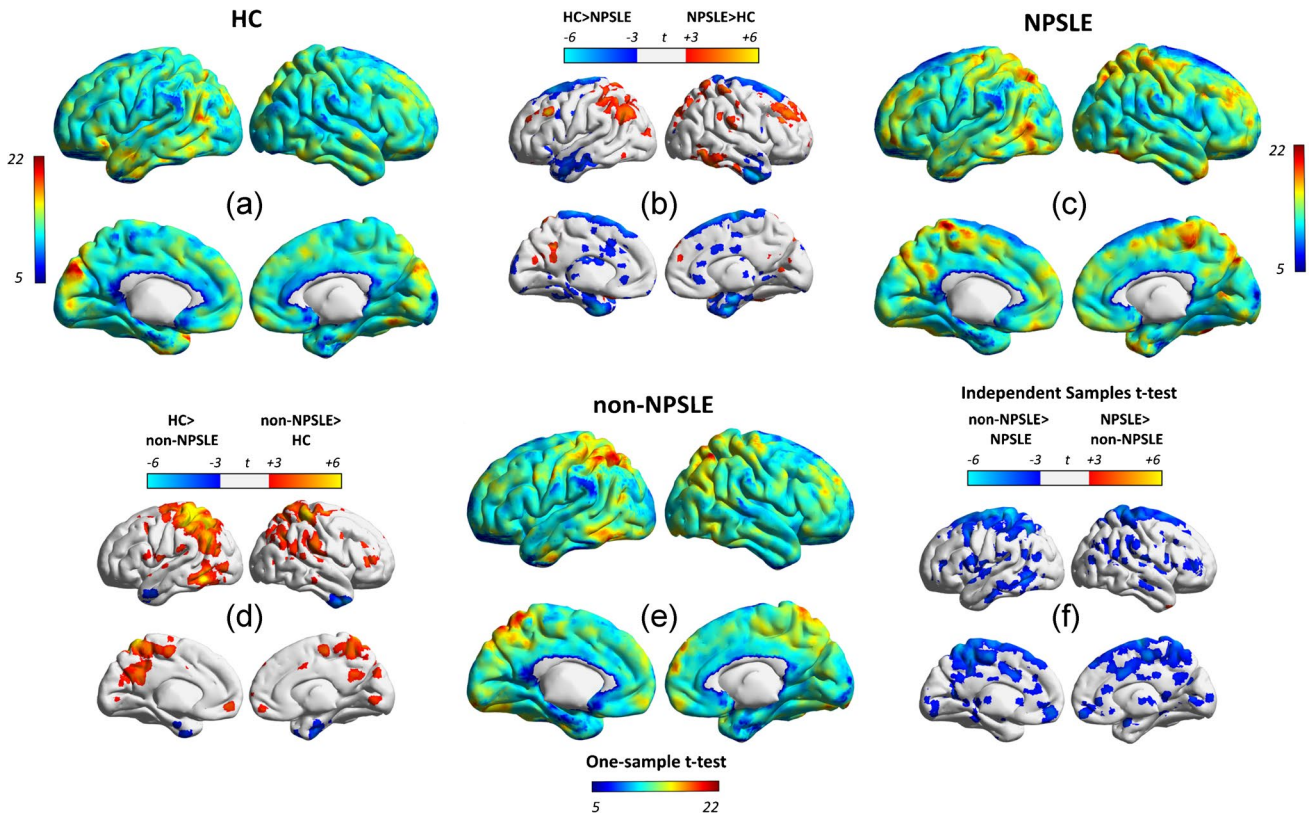


**Fig. 2** Whole-brain ICC maps. **a**, **c**, **e** One-sample *T* maps in the healthy control (HC), non-NPSLE, and NPSLE groups displaying voxels with significant ICC values. **b**, **d**, **f** Pairwise t-contrasts on parametric ICC maps between study groups. All tests were thresholded at $p < .05$, FDR corrected, with minimum cluster size of 200 voxels

**Functional connectivity-hemodynamic coupling** The percentage of voxels in the right SPL displaying ICC-hemodynamic uncoupling correlated *negatively* with several cognitive measures (controlling for age), namely, digits forward ($r = -.43$, $p = .01$), Digits Reverse ($r = -.55$, $p = .001$), AVLT Immediate Recall ($r = -.50$, $p = .01$), AVLT Delayed Recall ($r = -.53$, $p = .001$), Trail Making Test A ($r = -.42$, $p = .01$), and Trail Making Test B ($r = -.40$, $p = .01$). Conversely, the percentage of voxels displaying ICC-hemodynamic coupling in the right posterior middle temporal and angular gyri (which were also more predominant among NPSLE as compared to HC participants) correlated *positively* with performance, (AVLT Delayed Recall: $r = .42$, $p = .01$) and time to complete the Grooved Pegboard test ($r = -.40$, $p = .01$).

## Discussion

In the current study, a complex interplay between hemodynamic status and functional brain organization in SLE was found. Specifically, NPSLE patients demonstrated intrinsic hypoconnectivity in anterior DMN components and hyperconnectivity in posterior DMN components, as compared to healthy controls. These findings are in partial agreement with the limited number of rs-fMRI studies conducted in NPSLE patients [15, 19]. They are also in agreement with previous results from the same cohort of NPSLE patients, using a very different approach (machine learning) to identify connectivity hubs that optimally differentiate NPSLE patients and healthy volunteers [14]. Moreover, increased intrinsic connectivity in at least two posterior DMN components (precuneus and SPL) was paralleled by elevated hemodynamic lag, in agreement with an earlier report of our group showing reduced perfusion in the semioval center in NPSLE patients [6]. Such regional hypoperfusion may reflect prominent vasculopathy, diffuse chronic ischemia, and neuronal loss in this region [39]. The positive association of hemodynamic lag in some of these regions correlated positively with disease duration is consistent with the notion that possible perfusion disturbances emerge with advanced disease progression.

Hyperconnectivity in sensorimotor regions is also in agreement with the report of increased functional connectivity between and within the sensorimotor network, although both increased and decreased connectivity was

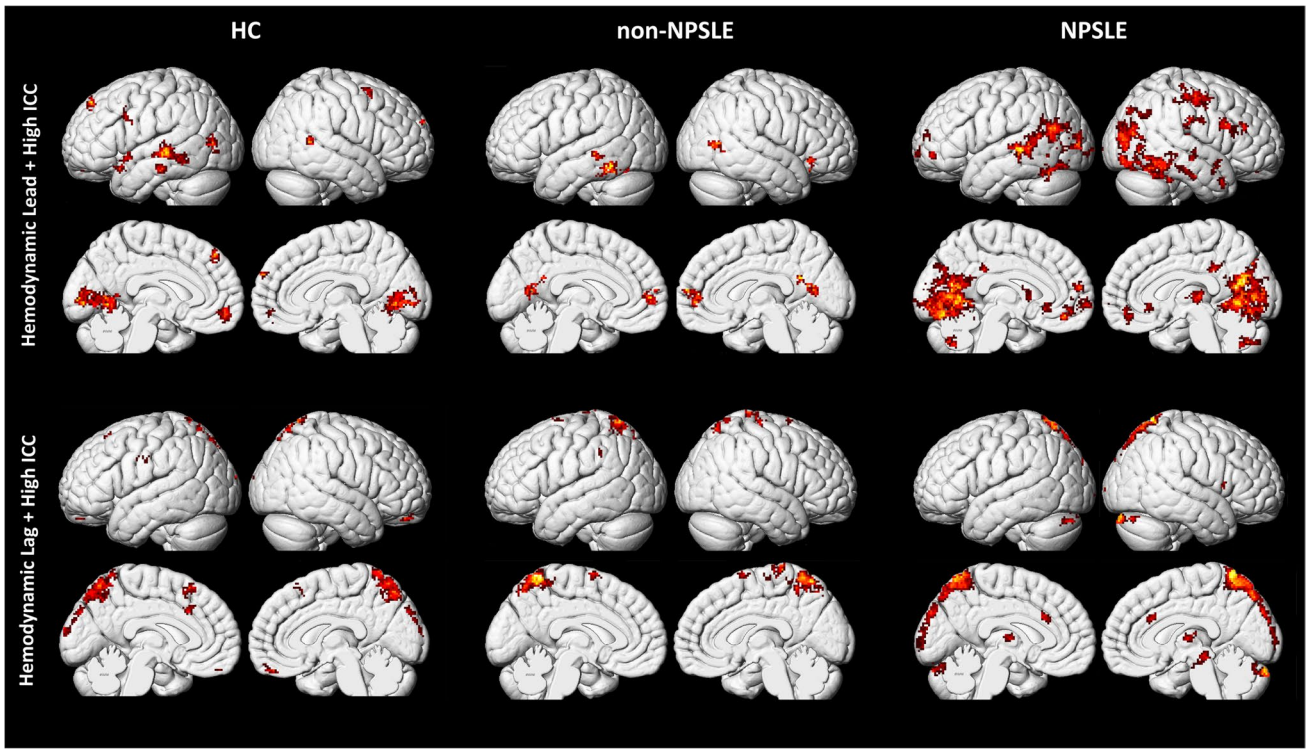


**Fig. 3** Connectivity-hemodynamic coupling in the group of healthy volunteers (HC), non-NPSLE, and NPSLE patients. Clusters of voxels that showed significantly elevated ICC ($p < .1$, FDR corrected in one-sample $t$ tests) combined with hemodynamic lead (TSA values $< -1$ TR) are plotted in the upper panels; clusters of voxels that showed significantly elevated ICC combined with hemodynamic lag (TSA values $> 1$ TR) are plotted in the lower panels

found with the DMN in that study [19]. A similar finding or increased DMN connectivity was also reported by Hou et al. [21] in a group of 30 non-NPSLE patients of comparable disease duration and disease activity. Our findings are also partly consistent with the findings of Zhang et al. [20] who reported increased degree centrality in anterior components of the DMN, albeit decreased functional connectivity in posterior portions of the DMN in non-NPSLE patients. It should be noted, however, that compared to the patient group studied by Zhang et al., our non-NPSLE sample comprised much older patients with longer disease duration who at the time of testing had much milder disease activity as indicated by their average SLEDAI score. It is noteworthy that hyperconnectivity and increased hemodynamic lag in posterior DMN regions in this group was also found in comparison to the NPSLE group that comprised patients with comparable disease duration and activity at the time of the fMRI scan. Despite their cross-sectional nature, these preliminary findings may suggest greater compensatory processes—possibly in response to concomitant, regional hemodynamic disturbance—in lupus patients who do not manifest neuropsychiatric symptoms. Moreover, our results may help explain the recent finding in this population of reduced capacity to suppress BOLD activity in posterior DMN regions during performance of cognitive tasks [40].

## Functional role of hemodynamic and connectivity changes in NPSLE

Another important finding of the present study concerns the potential clinical significance of changes in hemodynamics and functional connectivity in NPSLE. Specifically, relative hyperconnectivity of posterior (bilateral SPL) and anterior DMN components (right superior frontal gyrus) correlated positively with immediate verbal memory scores. Moreover, preserved (or even increased) hemodynamic-connectivity coupling in posterior components of the DMN (posterior middle temporal and angular gyrus in the right hemisphere) appears to be beneficial for diverse cognitive functions (immediate verbal memory and visuomotor coordination). Conversely, evidence of hemodynamic-connectivity uncoupling in posterior DMN regions (right SPL) may be detrimental for a range of cognitive functions, including verbal memory (immediate and delayed), visuomotor coordination, and mental flexibility. It is of note that this uncoupling also parallels disease activity as indicated by higher SLEDAI scores. Thus, hemodynamic impairment in NPSLE patients

could trigger a compensatory *increase* in functional connectivity in some regions, although changes in regional functional connectivity (i.e., hypoconnectivity in anterior DMN components or hyperconnectivity in the left angular gyrus) may occur in the absence of concomitant changes in hemodynamics.

Taken together, these findings highlight a complex mechanism of functional adaptation of the brain to the disease, whereby compensatory increases in intrinsic connectivity formed by both posterior and anterior DMN components may contribute to the preservation of cognitive capacity in NPSLE. Conversely, an imbalance between hemodynamic activity and function (to the extent that the latter is reflected in the degree of cross-regional communication) is related to both higher disease activity and worse cognitive performance. Although not directly comparable, these results are consistent with several, small-scale, fMRI studies revealing increased BOLD signal in prefrontal and parietal regions during performance of executive and working memory tasks in NPSLE [41].

### Study limitations and cautionary note

The present results should be interpreted with caution in view of certain study limitations. Thus, we had no data regarding internal carotid artery atherosclerosis, which might affect cerebral perfusion. Furthermore, the small sample size of the non-NPSLE group does not permit direct comparisons with previous studies on functional connectivity, especially in view of the highly heterogenous nature of the disease in terms of both inter- and intra-individual variability, associated in part with clinical and treatment variables. Although associations with clinical and neuropsychological test scores found in the present study indicate moderate effect size in most cases, they indicate that several additional factors play a critical role in determining cognitive performance, in addition to measurement error in both cognitive test scores and rs-fMRI recordings and derived indices. Along these lines, several confounders may have contributed to the observed statistical associations between TSA and ICC indices and cognitive measures. Among them, emotional disturbances, particularly depression symptoms, may have indirectly affected performance on neuropsychological tests. Moreover, structural changes not visible on conventional MRI sequences, such as subtle white matter disturbances, may underlie, at least in part, the observed associations. Furthermore, structural and/or functional changes could be accounted for to some extent by clinical variables, such as disease duration, disease activity, and organ damage. Such relationships were observed in the present study, although the current sample size did not permit testing of complex models to assess mediating or moderating effects of clinical (as well as emotional variables) on the association between cognitive performance and connectivity/hemodynamics.

Longitudinal data involving multiple measurements of multiscale data is forthcoming in order to establish causative links between clinical and psychometric indices of the impact of the disease and the evolution of changes in brain function in SLE patients. Even more, a rather liberal multiple comparison correction method (FDR) was applied in the analyses. Further studies with larger samples and more stringent statistical thresholds (based on family-wise error rate; FWE) are warranted to confirm our findings.

It is also important to note that perfusion indices reported in the present study were derived from the analysis of time-lags (or leads) in resting-state recordings across brain voxels. These measures of time shift in the phase of low-frequency BOLD oscillations are presumed to reflect hemodynamic transfer lag times and have been validated in cases of severe brain ischemia [22–28]. Apparently, perfusion indices derived from TSA of rs-fMRI data and relative cerebral blood flow estimated from using DSC-MRI provide complementary measures of cerebral perfusion that differ in many respects. Thus, the former provides voxel-based estimates of hemodynamic lag or lead times in both grey and underlying white matter regions, as compared to the average time series recorded from major venous structures, whereas the latter relies on expertly placed measurement ROIs within the normal appearing cerebral white matter.

## Conclusion

In conclusion, hemodynamic disturbances coupled with intrinsic connectivity changes were found in SLE patients with or without neuropsychiatric involvement, particularly in DMN components and sensorimotor regions, indicative of compensatory functional connectivity changes in response to hemodynamic impairment, most extensive in non-NPSLE. This functional adaptation of the brain positively affects verbal memory and visuomotor coordination skills of NPSLE patients, possibly contributing to the preservation of their cognitive capacity.

**Supplementary Information** The online version contains supplementary material available at https://doi.org/10.1007/s00234-022-02924-x.

**Author's contribution** Conceptualization: Efrosini Papadaki; Nicholas Simos

Methodology: Efrosini Papadaki; Nicholas Simos; Eleftherios Kavroulakis

Formal analysis and investigation: Nicholas Simos; Eleftherios Kavroulakis

Writing — original draft preparation: Efrosini Papadaki; Despina Antypa; Nicholas Simos

Writing — review and editing: Efrosini Papadaki; George Bertsias; Thomas Maris; Dimitrios Boumpas

Funding acquisition: Eleftherios Kavroulakis
Resources: George Bertsias; Antonis Fanouriakis; Prodromos Sidiropoulos
Supervision: Efrosini Papadaki; Dimitrios Boumpas

**Funding** Financial support for this work was provided by the Hellenic Foundation for Research and Innovation (H.F.R.I.) under the "2nd Call for H.F.R.I. Research Projects to support Post-Doctoral Researchers" (Project Number: 1220).

**Data availability** The computed metrics derived from resting state fMRI recordings will be available upon request.

## Compliance with ethical standards

**Competing interests** The authors have no competing interests to declare that are relevant to the content of this article.

**Ethical approval** The hospital review board approved this study and the procedure was thoroughly explained to all patients and volunteers who signed informed consent.

## References

1. Bertsias GK, Boumpas DT (2010) Pathogenesis, diagnosis and management of neuropsychiatric SLE manifestations. Nat Rev Rheumatol 6:358–367
2. Ainiala H, Loukkola J, Peltola J, Abady M, Shoenfeld Y, Zandman-Goddard G (2001) The prevalence of neuropsychiatric syndromes in systemic lupus erythematosus. Neurology. 57:496–500
3. Cohen D, Rijnink EC, Nabuurs RJA et al (2017) Brain histopathology in patients with systemic lupus erythematosus: identification of lesions associated with clinical neuropsychiatric lupus syndromes and the role of complement. Rheumatology 56:77–86
4. Emmer BJ, van Osch MJ, Wu O et al (2010) Perfusion MRI in neuropsychiatric systemic lupus erythemathosus. J Magn Reson Imaging 32:283–288
5. Zimny A, Szmyrka-Kaczmarek M, Szewczyk P et al (2014) In vivo evaluation of brain damage in the course of systemic lupus erythematosus using magnetic resonance spectroscopy, perfusion weighted and diffusion-tensor imaging. Lupus 23:10–19
6. Papadaki E, Fanouriakis A, Kavroulakis E et al (2018) Neuropsychiatric lupus or not? Cerebral hypoperfusion by perfusion-weighted MRI in normal-appearing white matter in primary neuropsychiatric lupus erythematosus. Ann Rheum Dis 77:441–448
7. Wang PI, Cagnoli PC, McCune WJ et al (2012) Perfusion-weighted MR imaging in cerebral lupus erythematosus. Acad Radiol 19:965–970
8. Gasparovic CM, Roldan CA, Sibbitt WL et al (2010) Elevated cerebral blood flow and volume in systemic lupus measured by dynamic susceptibility contrast magnetic resonance imaging. J Rheumatol 37:1834–1843
9. Jia J, Xie J, Li H et al (2019) Cerebral blood flow abnormalities in neuropsychiatric systemic lupus erythematosus. Lupus. 28(9):1128–1133. https://doi.org/10.1177/0961203319861677
10. Zhuo Z, Su L, Duan Y et al (2020) Different patterns of cerebral perfusion in SLE patients with and without neuropsychiatric manifestations. Hum Brain Mapp 41(3):755–766. https://doi.org/10.1002/hbm.24837
11. Cao ZY, Wang N, Jia JT et al (2021) Abnormal topological organization in systemic lupus erythematosus: a resting-state functional magnetic resonance imaging analysis. Brain Imag Behav 15:14–24. https://doi.org/10.1007/s11682-019-00228-y
12. Preziosa P, Rocca MA, Ramirez GA et al (2020) Structural and functional brain connectomes in patients with systemic lupus erythematosus. Eur J Neurol 27(1):113–1e2. https://doi.org/10.1111/ene.14041
13. Bonacchi R, Rocca MA, Ramirez GA et al (2020) Resting state network functional connectivity abnormalities in systemic lupus erythematosus: correlations with neuropsychiatric impairment. Mol Psychiatry. https://doi.org/10.1038/s41380-020-00907-z
14. Simos NJ, Dimitriadis SI, Kavroulakis E et al (2020) Quantitative identification of functional connectivity disturbances in neuropsychiatric lupus based on resting-state fMRI: a robust machine learning approach. Brain Sci 10(11):777. https://doi.org/10.3390/brainsci10110777
15. Nystedt J, Mannfolk P, Jönsen A, Nilsson P, Strandberg TO, Sundgren PC (2019) Functional connectivity changes in core resting state networks are associated with cognitive performance in systemic lupus erythematosus. J Comp Neurol 527(11):1837–1856
16. Yu H, Qiu X, Zhang YQ et al (2019) Abnormal amplitude of low frequency fluctuation and functional connectivity in non-neuropsychiatric systemic lupus erythematosus: a resting-state fMRI study. Neuroradiology. 61(3):331–340
17. Liu S, Cheng Y, Xie Z et al (2018) A conscious resting state fMRI study in SLE patients without major neuropsychiatric manifestations. Front Psychiatry 9:677
18. Niu C, Tan X, Liu X et al (2018) Cortical thickness reductions associate with abnormal resting-state functional connectivity in non-neuropsychiatric systemic lupus erythematosus. Brain Imaging Behav 12(3):674–684
19. Nystedt J, Mannfolk P, Jönsen A et al (2018) Functional connectivity changes in systemic lupus erythematosus: a resting-state study. Brain Connect 8(4):220–234
20. Zhang XD, Jiang XL, Cheng Z et al (2017) Decreased coupling between functional connectivity density and amplitude of low frequency fluctuation in non-neuropsychiatric systemic lupus erythematosus: a resting-stage functional MRI study. Mol Neurobiol 54(7):5225–5235
21. Hou J, Lin Y, Zhang W et al (2013) Abnormalities of frontal-parietal resting-state functional connectivity are related to disease activity in patients with systemic lupus erythematosus. PLoS One 8(9):e74530. https://doi.org/10.1371/journal.pone.0074530
22. Khalil AA, Ostwaldt A-C, Nierhaus T et al (2017) Relationship between changes in the temporal dynamics of the blood-oxygen-level-dependent signal and hypoperfusion in acute ischemic stroke. Stroke 48:925–931
23. Khalil AA, Villringer K, Filleböck V et al (2020) Non-invasive monitoring of longitudinal changes in cerebral hemodynamics in acute ischemic stroke using BOLD signal delay. J Cereb Blood Flow Metab 40:23–34
24. Lv Y, Margulies DS, Cameron Craddock R et al (2013) Identifying the perfusion deficit in acute stroke with resting-state functional magnetic resonance imaging. Ann Neurol 73:136–140
25. Tong Y, Lindsey KP, Hocke LM, Vitaliano G, Mintzopoulos D, Frederick BD (2017) Perfusion information extracted from resting state functional magnetic resonance imaging. J Cereb Blood Flow Metab 37:564–576
26. Mitra A, Snyder AZ, Hacker CD, Raichle ME (2014) Lag structure in resting-state fMRI. J Neurophysiol 111:2374–2391
27. Siegel JS, Snyder AZ, Ramsey L, Shulman GL, Corbetta M (2016) The effects of hemodynamic lag on functional connectivity and behavior after stroke. J Cereb Blood Flow Metab 36(12):2162–2176
28. Amemiya S, Kunimatsu A, Saito N, Ohtomo K (2014) Cerebral hemodynamic impairment: assessment with resting-state functional MR imaging. Radiology. 270(2):548–555

29. Yan S, Qi Z, An Y, Zhang M, Qian T, Lu J (2019) Detecting perfusion deficit in Alzheimer's disease and mild cognitive impairment patients by resting-state fMRI. J Magn Reson Imaging 49(4):1099–1104
30. Antypa D, Simos NJ, Kavroulakis E et al (2021) Anxiety and depression severity in neuropsychiatric SLE are associated with perfusion and functional connectivity changes of the frontolimbic neural circuit: a resting-state f(unctional) MRI study. Lupus Sci Med 8(1):e000473. https://doi.org/10.1136/lupus-2020-000473
31. Hochberg MC (1997) Updating the American College of Rheumatology revised criteria for the classification of systemic lupus erythematosus. Arthritis Rheum 40(9):1725–1725
32. Gladman DD, Ibañez D, Urowitz MB (2002) Systemic lupus erythematosus disease activity index 2000. J Rheumatol 29:288–291
33. Gladman DD, Goldsmith CH, Urowitz MB et al (2000) The Systemic Lupus International Collaborating Clinics/American College of Rheumatology (SLICC/ACR) damage index for systemic lupus erythematosus international comparison. J Rheumatol 27:373–376
34. (1999) The American College of Rheumatology nomenclature and case definitions for neuropsychiatric lupus syndromes. Arthritis Rheum 42:599–608
35. Whitefield-Gabrieli S, Nieto-Castanon A (2012 Jun) Conn: a functional connectivity toolbox for correlated and anticorrelated brain networks. Brain Connectivity 2(3):125–141
36. Layden E. Intrinsic_connectivity_contrast [Internet]. MATLAB Central File Exchange. 2020 [cited 2020 Apr 2]. Available from: https://ch.mathworks.com/matlabcentral/fileexchange/68248-intrinsic_connectivity_contrast
37. Slotnick SD (2017) Cluster success: fMRI inferences for spatial extent have acceptable false-positive rates. Cogn Neurosci 8:150–155
38. Slotnick SD, Moo LR, Segal JB, Hart J Jr (2003) Distinct prefrontal cortex activity associated with item memory and source memory for visual shapes. Brain Res Cogn Brain Res 17:75–82
39. Wiseman SJ, Bastin ME, Jardine CL et al (2016) Cerebral small vessel disease burden is increased in systemic lupus erythematosus. Stroke 47:2722–2728
40. Barraclough M, McKie S, Parker B et al (2019) Altered cognitive function in systemic lupus erythematosus and associations with inflammation and functional and structural brain changes. Ann Rheum Dis 78(7):934–940
41. Mikdashi JA (2016) Altered functional neuronal activity in neuropsychiatric lupus: a systematic review of the fMRI investigations. Semin Arthritis Rheum 45(4):455–462




## Authors and Affiliations


**Efrosini Papadaki[1,2] · Nicholas J. Simos[2,3] · Eleftherios Kavroulakis[1] · George Bertsias[4,5] · Despina Antypa[6] · Antonis Fanouriakis[4,7] · Thomas Maris[1,2] · Prodromos Sidiropoulos[4] · Dimitrios T Boumpas[4,7,8,9]**

1 Department of Radiology, School of Medicine, University of Crete, University Hospital of Heraklion, 71003 Heraklion, Crete, Greece

2 Computational Bio-Medicine Laboratory, Institute of Computer Science, Foundation for Research and Technology – Hellas, Heraklion, Greece

3 Department of Electrical and Computer Engineering, Technical University of Crete, Chania, Crete, Greece

4 Department of Rheumatology, Clinical Immunology and Allergy, School of Medicine, University of Crete, University Hospital of Heraklion, Heraklion, Crete, Greece

5 Institute of Molecular Biology and Biotechnology, Foundation of Research and Technology-Hellas, Voutes, Heraklion, Greece

6 Department of Psychiatry, School of Medicine, University of Crete, University Hospital of Heraklion, Heraklion, Crete, Greece

7 4th Department of Internal Medicine, Attikon University Hospital, Medical School, National and Kapodestrian University of Athens, Athens, Greece

8 Laboratory of Autoimmunity and Inflammation, Biomedical Research Foundation of the Academy of Athens, Athens, Greece

9 Joint Academic Rheumatology Program, and 4th Department of Medicine, Medical School, National and Kapodestrian University of Athens, Athens, Greece